Supporting Information

GRPR–targeted SPECT imaging using a novel bombesin-based peptide for colorectal cancer detection

*Peifei Liu[#] [a], Yuanbiao Tu[#] [a,b], Ji Tao [a], Zicun liu [a], Fang Wang [a], Yi Ma [a], Zhaolun Li [a], Zhihao Han [a], and Yueqing Gu [*a]*

[#] These authors contributed equally to the work

** Corresponding author*

[a] *State Key Laboratory of Natural Medicine, Department of Biomedical Engineering, School of Engineering, China Pharmaceutical University, No. 24 Tongjia Lane, Gulou District, Nanjing 210009, China*

E-mail: *guengineering@cpu.edu.cn*

[b] *Jiangzhong Cancer Research Center, Jiangxi University of Traditional Chinese Medicine, No.1688 Meiling Road, Wanli District, Nanchang 330004, China.*

MPA: ^{1}H NMR (400 MHz, D_2O) δ 8.76 (d, *J* = 13.7 Hz, 2H), 7.79 (s, 2H), 7.73 (d, *J* = 8.3 Hz, 2H), 7.27 (d, *J* = 8.4 Hz, 2H), 6.27 (d, *J* = 18.6 Hz, 2H), 4.20 (dd, *J* = 9.8, 4.8 Hz, 4H), 2.96 (t, *J* = 7.0 Hz, 5H), 2.82 (t, *J* = 7.1 Hz, 2H), 2.60-2.53 (m, H), 2.49 (t, *J* = 7.0 Hz, 2H), 2.36 (t, *J* = 7.0 Hz, 2H), 2.24-2.09 (m, 4H), 1.86-1.63 (m, 12H).

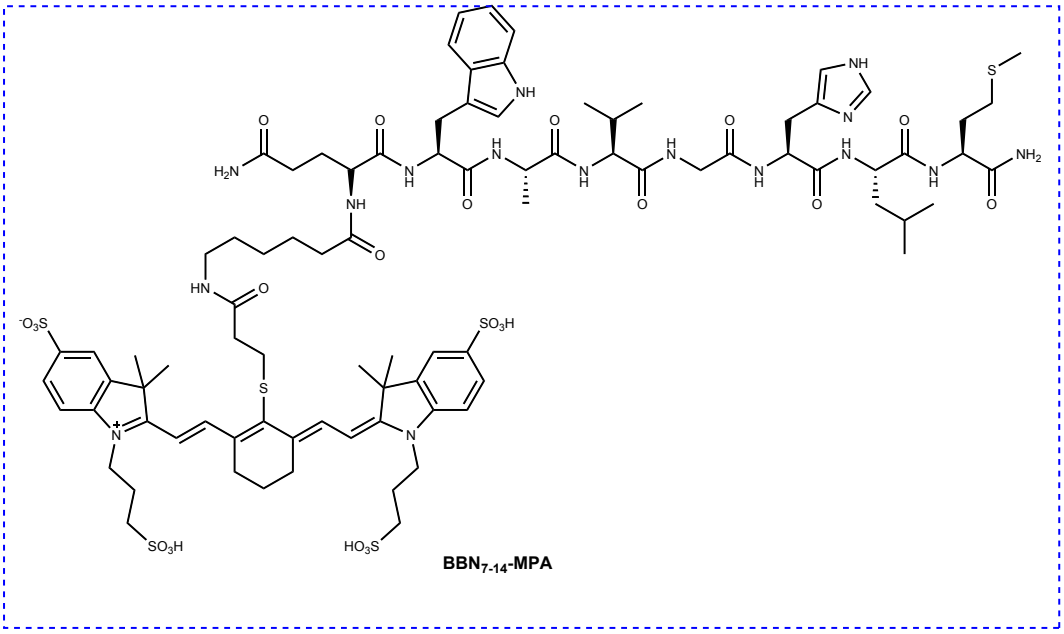

Figure S1-1. The chemical structures of BBN_{7-14}-MPA

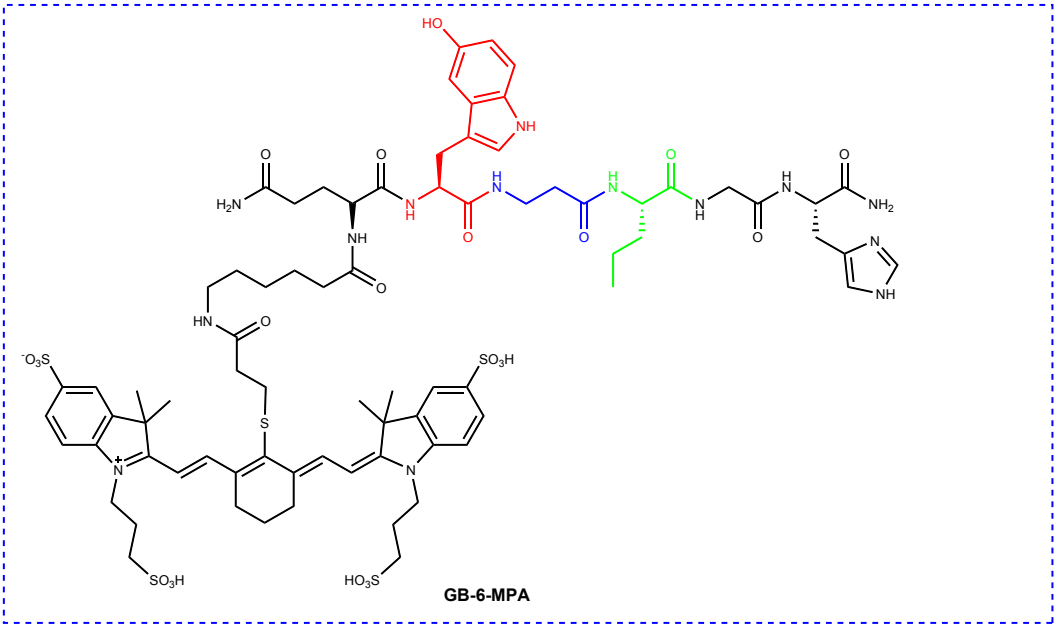

Figure S1-2. The chemical structures of GB-6-MPA

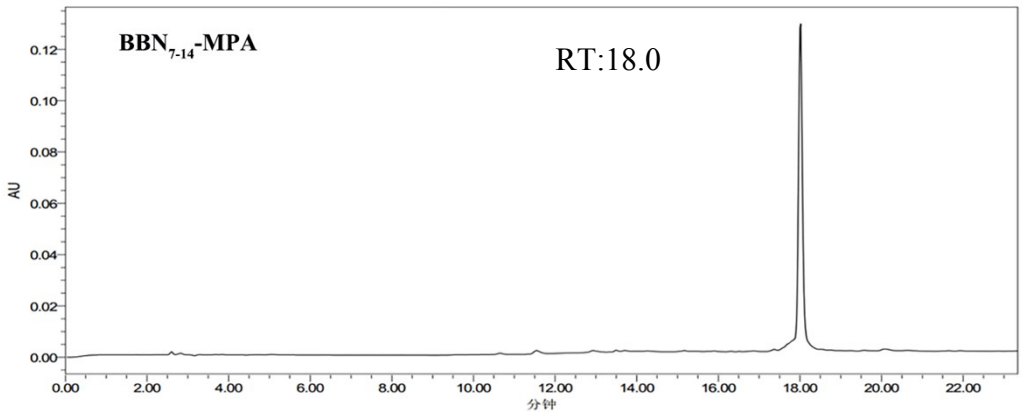

Figure S1-3. Typical HPLC chromate-gram of BBN_{7-14}-MPA. (RT: retention time)

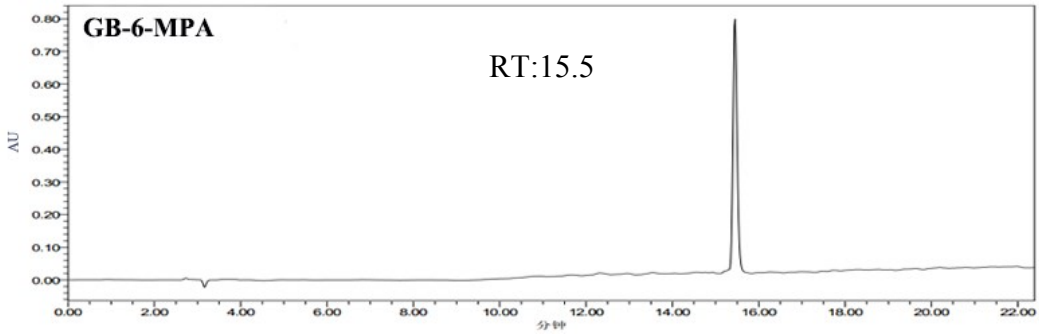

Figure S1-4. Typical HPLC chromate-gram of GB-6-MPA. (RT: retention time)

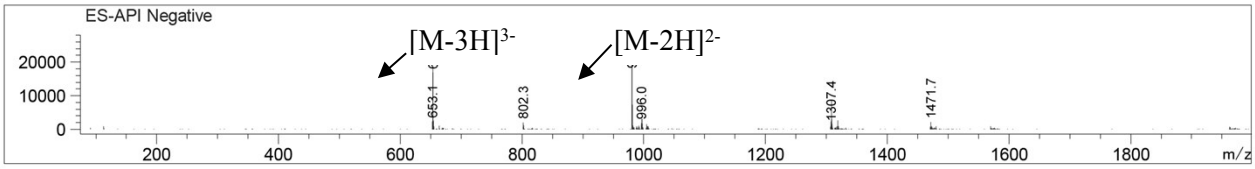

Figure S1-5. MS spectrum of BBN_{7-14}-MPA (MW:1965.42)

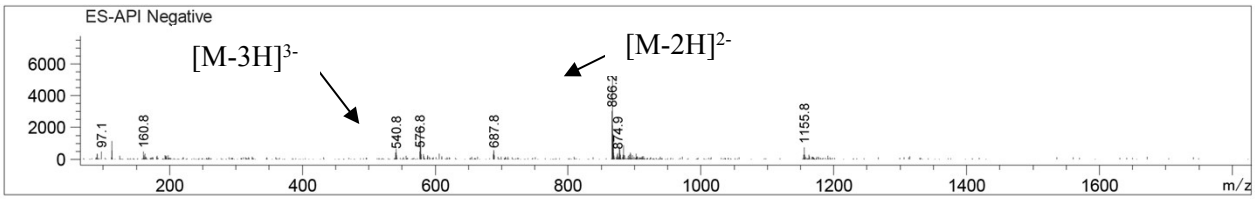

Figure S1-6. MS spectrum of GB-6-MPA (MW:1736.06)

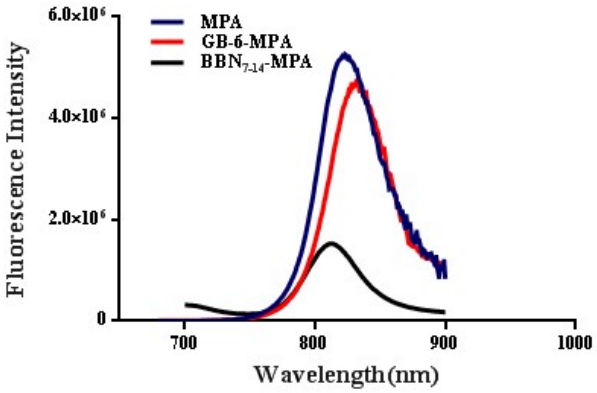

Figure S1-7. fluorescence spectra of free MPA, GB-6-MPA and BBN_{7-14}-MPA, respectively.

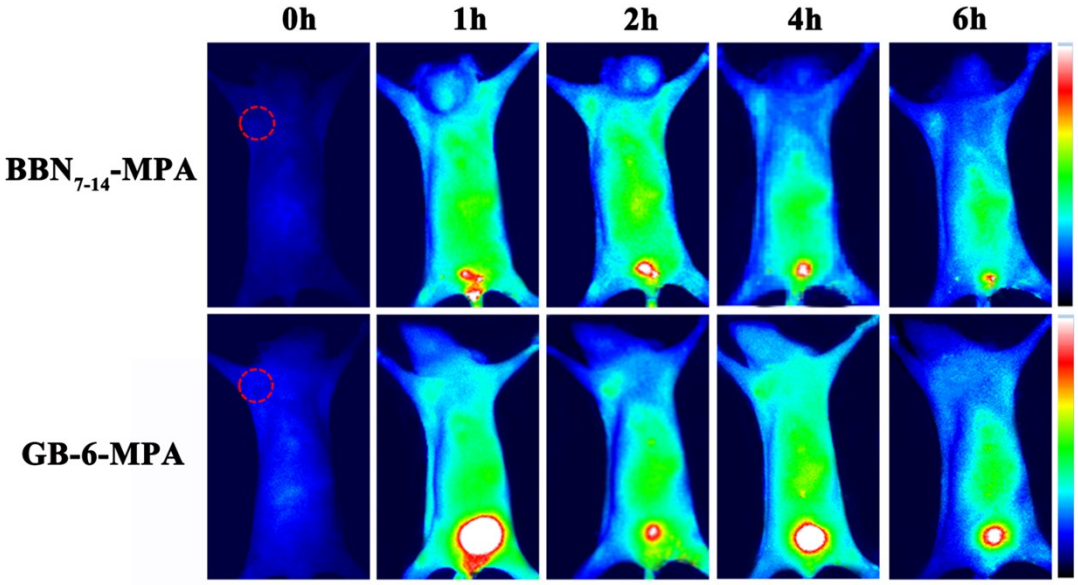

Figure S1-8 *in vivo* imaging of BBN_{7-14}–MPA and GB-6-MPA in mice bearing HeLa tumors at different times. (The position of the tumor was indicated by a red dashed-dotted circle.)

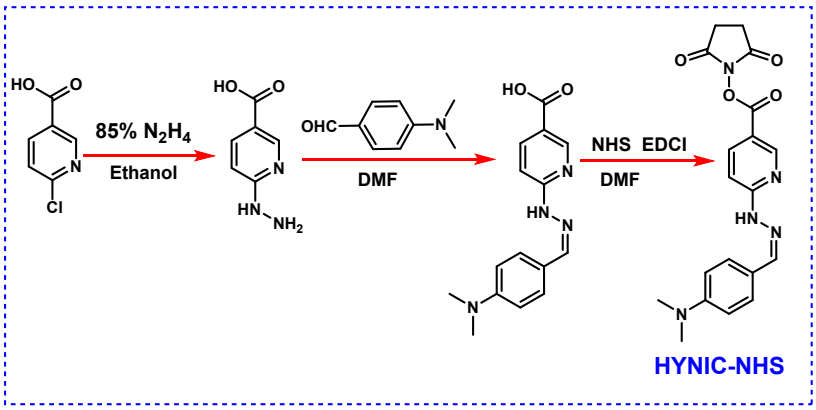

Figure S2-1. Structure and synthetic route of HYNIC-NHS

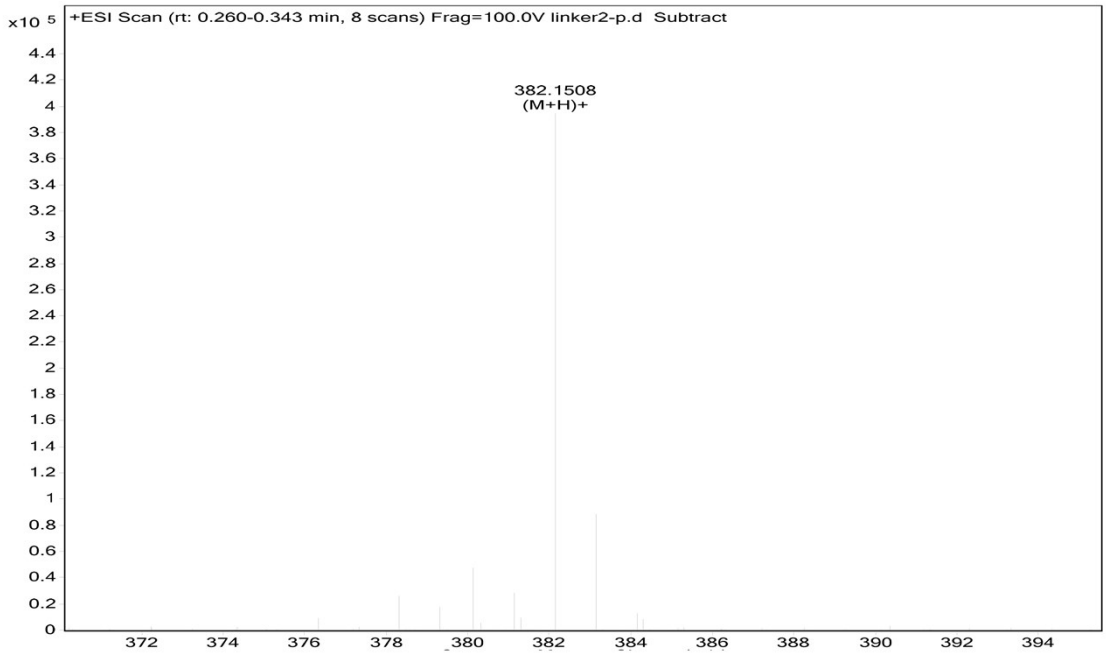

Figure S2-2. MS spectrum of HYNIC-NHS (MW:381.39)

HYNIC-NHS: 1H NMR (400 MHz, DMSO-d) δ 8.60 (s, 1H), 8.08 (d, J = 7.5 Hz, 1H), 7.99 (s, 1H), 7.51 (d, J = 7.3 Hz, 2H), 7.40 (d, J = 7.5 Hz, 1H), 6.71 (d, J = 7.6 Hz, 2H), 3.01 (s, 6H), 2.78 (s, 4H).

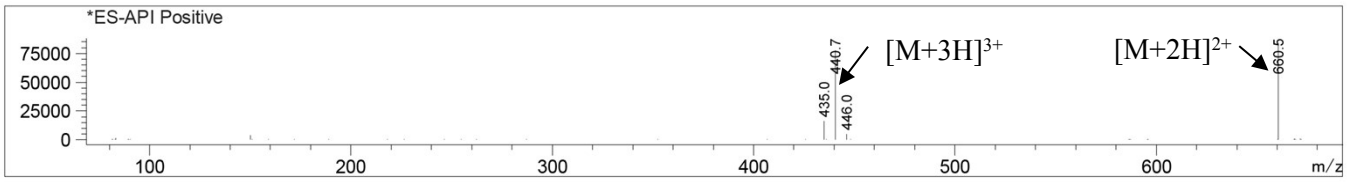

Figure S2-3. MS spectrum of HYNIC-BBN_{7-14} (MW:1319.66)

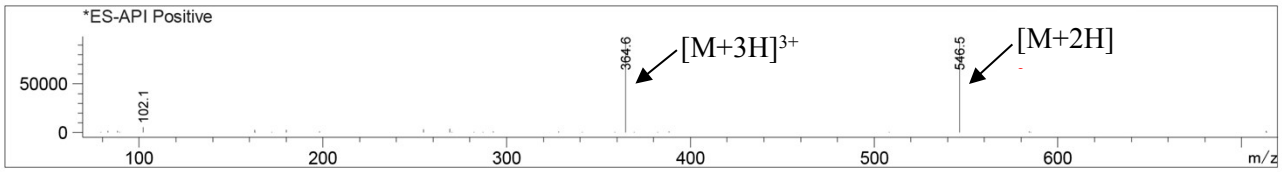

Figure S2-4. MS spectrum of HYNIC-GB-6 (MW:1091.23)

Radiochemistry

HYNIC-BBN_{7-14} and HYNIC-GB-6 were prepared by direct conjugation of Aca-BBN_{7-14} or Aca-GB-6 with HYNIC-NHS (Figure S2-1), respectively. The products were confirmed by C18 analytical HPLC (purity

>98%). The molecule weight of HYNIC-BBN_{7-14} was corroborated by mass spectrometry ($[M+2H]^{2+}$=660.5 and ($[M+3H]^{3+}$=440.7) and matches with calculated value (1319.66) (Figure S3-3). The mass measured molecule weight of HYNIC-GB-6 ($[M+2H]^{2+}$=613.5 and ($[M+3H]^{3+}$= 409.4) and was consistent with the expected molecule weight (1225.39). HYNIC- BBN_{7-14} and HYNIC-GB-6 were radiolabeled with $Na^{99m}TcO_4$ through a reported method, using TPPTS and tricine as coligands to obtain highly stable complexes with a yield of >96% and specific activity of >25 GBq/μmol. Subsequent, the tracers were purified via a Sep-Pak C-18 column and improved the radiochemical purity of the tracers to >99%. The Radio-HPLC chromatography of the purified tracers are shown in Figure S2-5. The well-prepared probe was used for further experiments, without further purification.

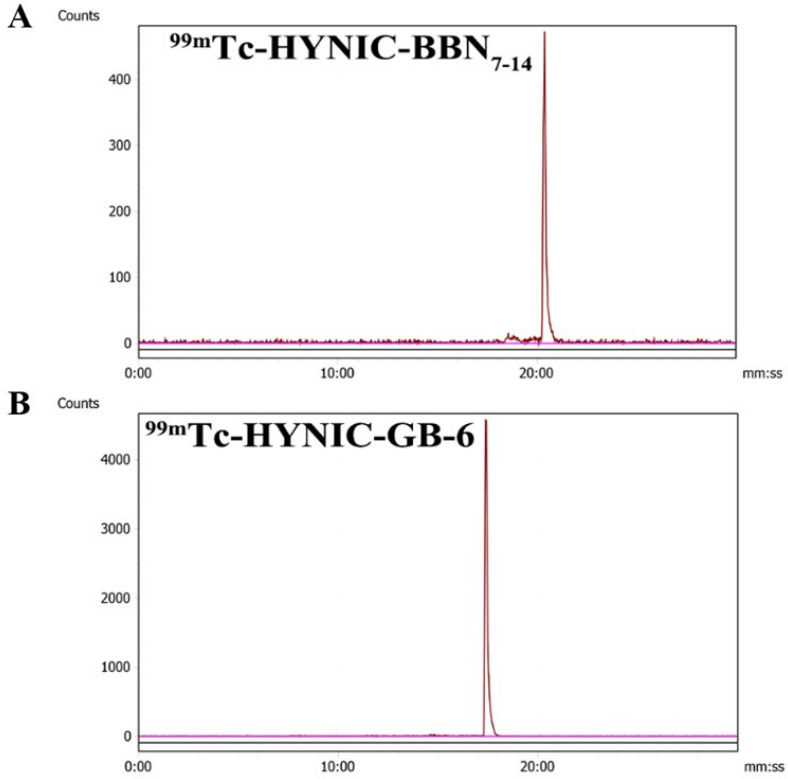

Figure S2-5. Typical radio-HPLC chromate-gram of ^{99m}Tc-radiolabeled compounds.

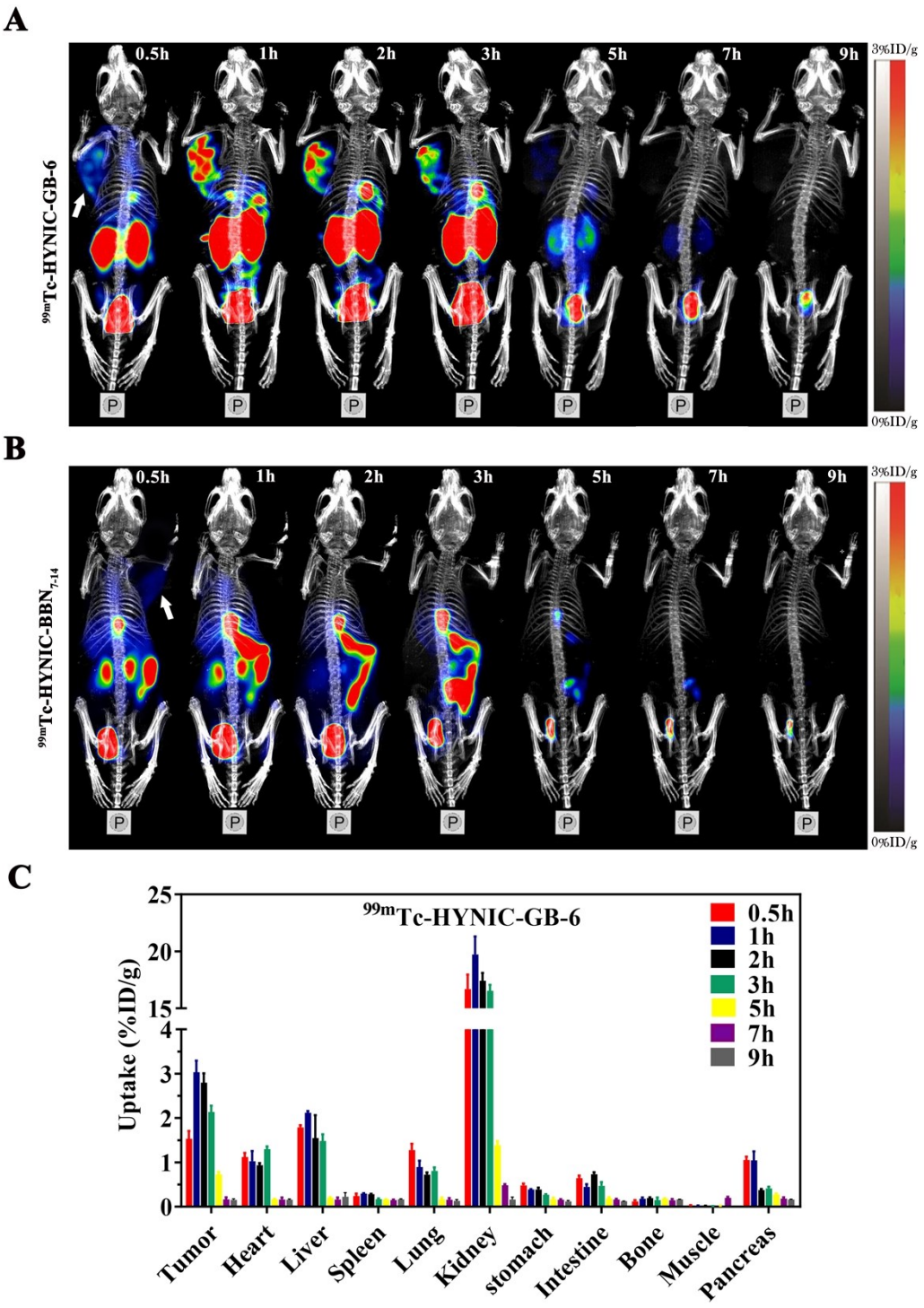

Figure S3. The images using small-animal SPECT-CT and biodistribution using γ-counter. (A) Representative SPECT-CT images of subcutaneous Caco-2 xenograft model acquired at 0.5 h, 1 h, 2 h, 3 h, 5 h, 7 h and 9 h after ^{99m}Tc-HYNIC-GB-6 injection (n = 3) in the posterior (P) view and the white arrow indicates the location of the tumor. (B) SPECT-CT images of subcutaneous Caco-2 xenograft models acquired at 0.5 h, 1 h, 2 h, 3 h, 5 h, 7 h and 9 h after ^{99m}Tc-HYNIC-BBN$_{7–14}$ injections (n = 3) in the posterior (P) view and the white arrow points out the tumor site. (C) Biodistribution of ^{99m}Tc-HYNIC-GB-6 (n= 3) in tumor and multiple organs of Caco-2 tumor bearing nude mice at different time points after administration (mean ± SD)

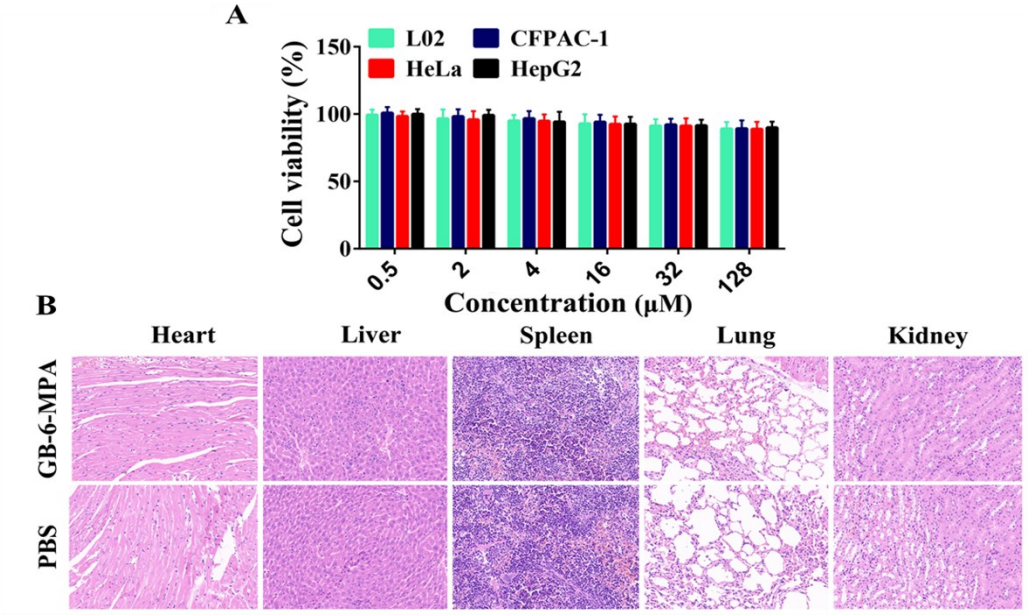

Figure S4 Cell viability assay *in vitro* and toxicity assay *in vivo* of GB-6-MPA. (A) The cell viability of GB-6-MPA in L02, CFPAC-1, HeLa and HepG2 were examined by MTT assay. (B) Acute toxicity was tested in mice and H&E staining was used to stain the excised organs observed for H&E analysis. Cell viability assay was carried out in order to investigate the in *vitro* toxicity after treatment of GB-6-MPA for 4 h with different concentrations on L02, CFPAC-1, HeLa and HepG2 cell lines. No significant toxic effect to the four cell lines were observed upon treatment with GB-6-MPA at any concentration for 4 h, with a percentage of viability of over 80.0% (Figure S4A). Further, acute toxicity was tested in *vivo* model by tail vein injection. H&E staining was used to stain the excised organs including heart, liver, spleen, lung and kidney observed for H&E analysis after the acute toxicity experiment (Figure S4B). We evaluated the histological examination results and found no drug toxicity, infection, or organ damage in GB-6-MPA groups as compared with PBS control group (*Biomater. Sci., 2020, 8, 2682*).

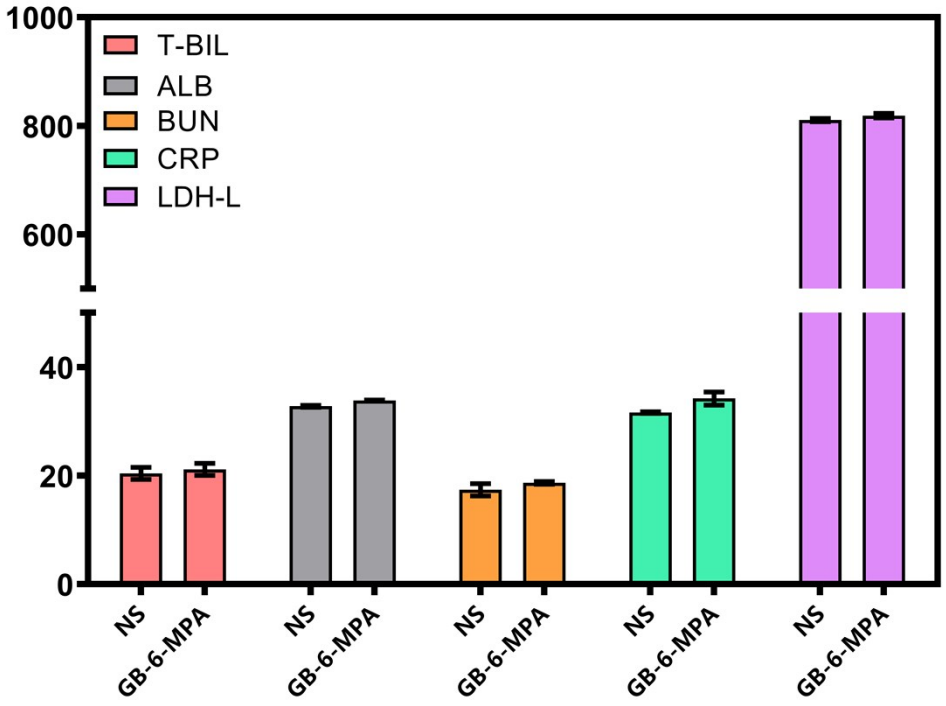

Figure S5. Analysis of blood biochemical parameters. A biochemical analysis of blood serum parameters was performed. ICR mice were randomly divided into two groups with each group comprising of four mice: a control group and GB-6-MPA treatment group. Mice in experimental group were administered of GB-6-MPA by intravenous administration at 10mg/1kg daily for 14 days. And control mice were treated with normal saline (NS). On the 15th day, the animals were sacrificed, after being anesthetized with ether, to enable further assessment of the biochemical parameters (*Theranostics, 2020; 10(9):4073-4087*). The result showed that total bilirubin (T-BIL), albumin (ALB), blood urea nitrogen (BUN), aspartate creactiveprotein (CRP) and lactic dehydrogenase (LDH-L) levels did not differ significantly between the experimental and control groups. Total bilirubin (T-BIL) and albumin (ALB) are related to the liver function. Blood urea nitrogen (BUN) and aspartate creactiveprotein (CRP) are associated with kidney function. And The plasma activity of lactate dehydrogenase (LDH) served as a general indicator of cell injury. None of these markers differed from the control levels for the same observation periods.